

Model for fluorescence quenching in light harvesting complex II in different aggregation states

Atanaska Andreeva · Silvia Abarova ·
Katerina Stoitchkova · Mira Busheva

Received: 8 May 2008 / Revised: 9 September 2008 / Accepted: 10 September 2008 / Published online: 26 September 2008
© European Biophysical Societies' Association 2008

Abstract Low-temperature (77 K) steady-state fluorescence emission spectroscopy and dynamic light scattering were applied to the main chlorophyll *a/b* protein light harvesting complex of photosystem II (LHC II) in different aggregation states to elucidate the mechanism of fluorescence quenching within LHC II oligomers. Evidences presented that LHC II oligomers are heterogeneous and consist of large and small particles with different fluorescence yield. At intermediate detergent concentrations the mean size of the small particles is similar to that of trimers, while the size of large particles is comparable to that of aggregated trimers without added detergent. It is suggested that in small particles and trimers the emitter is monomeric chlorophyll, whereas in large aggregates there is also another emitter, which is a poorly fluorescing chlorophyll associate. A model, describing populations of antenna chlorophyll molecules in small and large aggregates in their ground and first singlet excited states, is considered. The model enables us to obtain the ratio of the singlet excited-state lifetimes in small and large particles, the relative amount of chlorophyll molecules in large particles, and the amount of quenchers as a function of the degree of aggregation. These dependencies reveal that the quenching of the chl *a* fluorescence upon aggregation is due to the formation of large aggregates and the increasing of the amount of chlorophyll molecules forming these aggregates.

As a consequence, the amount of quenchers, located in large aggregates, is increased, and their singlet excited-state lifetimes steeply decrease.

Keywords Light harvesting complex II · 77 K chlorophyll fluorescence · Aggregation · Fluorescence quenching

Abbreviations

LHC II	Main chlorophyll <i>a/b</i> protein light harvesting complex of photosystem II
chl	Chlorophyll
NPQ	Non-photochemical quenching
DM	<i>n</i> -Dodecyl β -D-maltoside
CMC	Critical micelle concentration
F680	Fluorescence band at 680 nm
F700	Fluorescence band at 698 nm

Introduction

The main light-harvesting antenna complex of photosystem II (LHC II) is a pigment–lipid–protein structure where light harvesting and light dissipation are closely related processes (Jansson 2005). Dissipation of the excess light energy as heat is accomplished by quenching of excited chlorophyll (chl) *a* singlet states, a mechanism referred to as non-photochemical quenching (NPQ). The precise molecular mechanisms of NPQ still remain controversial (Holt et al. 2005; Finazzi et al. 2004; Standfuss et al. 2005; Pascal et al. 2005; Cseh et al. 2000; Van Oort et al. 2007a, b; Grudziński et al. 2002).

Recently, the structure of spinach and pea LHC II was resolved at resolution of 2.72 Å (Liu et al. 2004) and of 2.5 Å (Standfuss et al. 2005) by X-ray crystallography. An

A. Andreeva (✉) · S. Abarova · K. Stoitchkova
Department of Condensed Matter Physics, Faculty of Physics,
Sofia University, 5, J. Bourchier blvd., 1164 Sofia, Bulgaria
e-mail: andreeva@phys.uni-sofia.bg

M. Busheva
Institute of Biophysics, Bulgarian Academy of Sciences,
Acad. G. Bonchev str. bl.21, 1113 Sofia, Bulgaria

atomic model for the LHC II was proposed which constituted an important step for correlating the structure to the spectroscopic properties. It revealed the mutual arrangement of 42 chlorophylls, from which 24 are chl *a* and 18 chl *b*, 12 carotenoids and 6 lipids in LHC II trimer. In vivo, most of the complexes are trimeric, but variation in the degree of aggregation of LHC II also occurs and is related to NPQ (Horton et al. 1996).

The trimeric LHC II is highly fluorescing thus indicating a low rate of energy dissipation. When LHC II forms aggregates, strong chlorophyll fluorescence quenching occurs (Pascal et al. 2005; Van Oort et al. 2007a; Vasil'ev et al. 1997; Huyer et al. 2004; Palacios et al. 2002; Moya et al. 2001; Mullineaux et al. 1993; Barzda et al. 2001; Gilmore et al. 1995). The increase in energy dissipation within LHC II oligomers compared to trimers provides a model for understanding in vivo NPQ because of the strong similarity between these two processes. The understanding of the molecular mechanism of the fluorescence quenching will help us to get an insight into the molecular mechanism of NPQ.

At 77 K the lifetime of trimeric LHC II excited state is relatively long (Vasil'ev et al. 1997; Huyer et al. 2004; Palacios et al. 2002; Moya et al. 2001; Mullineaux et al. 1993; Barzda et al. 2000). The values of its average lifetime are typically around 4–5 ns being scattered from 5.4 ns (Vassil'ev et al. 1997; Huyer et al. 2004), 5.18 ns (Palacios et al. 2002), 4.8 ns (Moya et al. 2001) to 4.3 ns (Mullineaux et al. 1993) and 4.1 ns (Barzda et al. 2000). Although two components were usually observed in 77 K chl *a* fluorescence decay, slow and fast, most of the chlorophyll *a* fluorescence is emitted from the slow decaying component (Van Oort et al. 2007a; Vasil'ev et al. 1997; Huyer et al. 2004; Palacios et al. 2002; Moya et al. 2001; Mullineaux et al. 1993). In the case of trimeric LHC II the short-lived component had a small contribution—only 1% in (Palacios et al. 2002), 10% in (Vasil'ev et al. 1997), 15% in (Huyer et al. 2004), and 22% in (Moya et al. 2001).

Divergent results from different laboratories about lifetimes of LHC II illustrate the complexity of their correct estimation. Moreover, the differences may be due to distinct plant species, different isolations and/or differences in chl *a* concentration. Possibly, some aggregation in the trimeric LHC II also explains the observation of multiexponential decays in the cited studies.

In LHC II aggregates the strong fluorescence quenching is concomitant with a shortening of the lifetime (Pascal et al. 2005; Vasil'ev et al. 1997; Huyer et al. 2004; Moya et al. 2001; Mullineaux et al. 1993; Van Oort et al. 2007a, b). At 80 K upon aggregation the main decay lifetime becomes about 0.11 ns (Mullineaux et al. 1993). In LHC II liposomes at 77 K four lifetimes are resolved ranging from 0.32 to 5.3 ns (Moya et al. 2001). According to Pascal et al.

(2005) the lifetime was remarkably uniform within the LHC II crystals—0.89 ns, and in the aggregated LHC II it was 0.65 ns.

To elucidate the molecular basis of fluorescence quenching phenomena a low-temperature (77 K) steady-state fluorescence emission spectroscopy and dynamic light scattering (Malvern system) were applied to LHC II in different aggregation states. The aim was to propose a model for the fluorescence quenching within LHC II oligomers, based on the recently resolved structure of LHC II at 2.72 Å (Liu et al. 2004) and at 2.5 Å (Standfuss et al. 2005) resolution by X-ray crystallography.

Materials and methods

Sample preparation

LHC II was isolated from leaves of market spinach as described earlier (Simidjiev et al. 1997) and washed twice in 20 mM Tricine (pH 7.8) buffer. The samples were suspended in the buffer with 40% glycerol. The aggregation state of the complexes was varied by adding of different concentrations of the detergent *n*-dodecyl β -D-maltoside (DM). The chlorophyll content of the samples, estimated by using the method of Lichtenthaler (1987), was adjusted to 10 μ g/ml. To normalize the emission spectra of LHC II, 1 μ M fluorescein (sodium salt) was added as an internal standard to the medium. At this concentration the fluorescein did not interfere with the chl *a* fluorescence emission (Krause et al. 1983). The addition of DM at the used concentrations did not change the fluorescence intensity of the fluorescein.

77 K chlorophyll fluorescence measurements

The 77 K chlorophyll fluorescence emission spectra were obtained in a translucent Dewar using a double monochromator spectrometer (model 1403, Spex) as described earlier (Andreeva et al. 2003). Excitation was provided by an argon ion laser (Inova 307) at 488 and 514.5 nm.

The 77 K chlorophyll fluorescence emission spectra excited at 436 nm were measured using a JobinYvon JY3 spectrofluorimeter. The actinic light with low enough intensity was provided by Xenon lamp “Suprasil” 150 W, the width of the slits being 4 nm.

The experimental spectra were corrected for the spectral sensitivity of the detection system.

Light scattering measurements

The size of the aggregates was determined by dynamic light scattering Malvern system-3600 equipped with a

64-channel correlator and Ar laser (488 nm) at a 90° angle. The temperature was $25 \pm 0.1^\circ\text{C}$. The medium and the chlorophyll content were the same as those for the fluorescence measurements.

Results and discussion

Experimental data

The preparations of LHC II isolated according to the procedure of Simidjiev et al. (1997) formed large aggregates. The critical micelle concentration (CMC) of DM, the concentration at which LHC II aggregates are disassembled into trimers, was about 0.02% (w/v). Low-temperature chl *a* emission spectra of DM treated LHC II are presented in Fig. 1. Excitation was performed at 436, 488 and 514.5 nm wavelengths, coinciding with the predominant absorption of chl *a*, chl *b*/neoxanthin and lutein molecules, respectively (Ruban et al. 2001). Fluorescence spectrum of trimeric LHC II (curve 5 in Fig. 1a) manifests typical characteristics of LHC II trimers—maximum at 680 nm (F680) and satellite vibrational peak at 740 nm. Its spectral shape is independent of the excitation wavelength, checked with the samples used in our experiments (data not shown). Below the CMC, the aggregation of the complexes caused the quenching of the chl *a* fluorescence (curves 1, 2, 3 and 4 in Fig. 1a). The quenching is concomitant with a strong broadening of the emission spectra and appearance of a new emission band (F700), considerably red-shifted compared to the emission spectrum of the trimeric forms of the LHC II (Ruban et al. 1997). This becomes particularly clear from Fig. 1b where spectra were normalized to their maxima. As can be seen, the first maximum at 680 nm of the spectra of aggregated complexes (curves 1, 2, 3, 4) is only slightly red-shifted, mainly due to the different ratio of the corresponding main bands amplitudes and especially to the increasing amplitude of F700. This indicates that the band at 680 nm presented in all samples has nearly the same band shape as the fluorescence spectrum of trimeric LHC II. A decomposition of the spectra with two main Gaussian bands and a third one—a shell of the vibrational subbands of the main bands, made for all steady-state fluorescence emission spectra, confirmed the above indication. All parameters were free-running and a very good fit was obtained using the curvefit program included in the packaged Lab calc, Arithmetic A2.23 (Galactic Ind. Corp.) programs (data not shown). Only a small shift in the position of F680 (about 1 nm) was observed, whereas the position of F700 was considerably red shifted.

Some emission contribution seems to be present around 700 nm even in trimers. As Palacios et al. (2002) have shown the spectral shapes of LHC II trimers and of chl *a* in

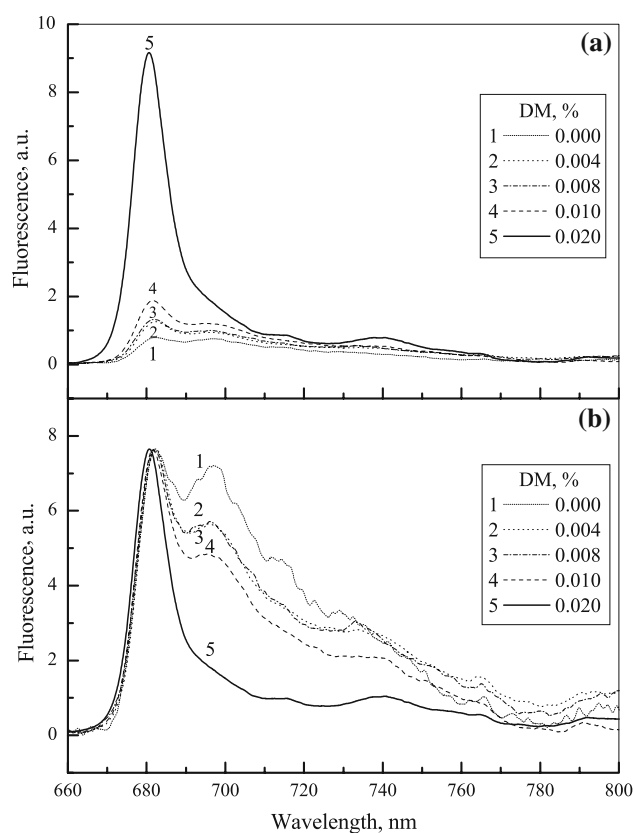


Fig. 1 77 K fluorescence spectra of LHC II at different DM concentrations (a) and the same spectra, normalized to their maxima (b). Fluorescence was excited at 436 nm. The spectral resolution was 4 nm

solution are identical, only red shifted. Analyzing the absorption spectrum of chl *a* monomer in solution in the red region, Shipman et al. (1976) have obtained that the Q_y transition is split into two discrete peaks at 659 nm $Q_y(0,0)$ and 613 nm $Q_y(0,1)$. We observed that the 77 K fluorescence emission spectral shape of LHC II trimers peaks at 679 nm (curve 5 in Fig. 1), as it was shown before (Hemerlrijk et al. 1992; Ruban et al. 1992, 1997). It coincides with the slightly red-shifted lineshape of chl *a* in solution, peaking at 678 nm at the same temperature (Boardman and Thorne 1971). The fluorescence emission spectrum, being a mirror image of the absorption spectrum is also split in this spectral region into two peaks, one main peaking at 679 nm and the other—vibronic one at 689 nm. So, the emission, seeming to contribute around 700 nm in trimers (obtained with 0.02% DM), is really presented, but it is located at 689 nm and is vibronic, emitted from the monomeric chl *a*.

Similar changes in the fluorescence intensity and spectral shapes with the decrease of detergent concentration were observed at all used excitation wavelengths. In the spectral shapes of emission, excited at different wavelengths, some differences exist as shown in Fig. 2,

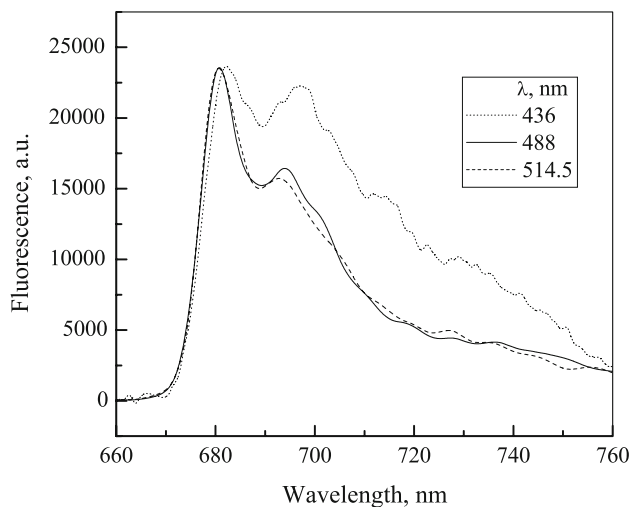


Fig. 2 Comparison of the normalized to the fluorescence maximum spectra of aggregated LHC II under different excitations

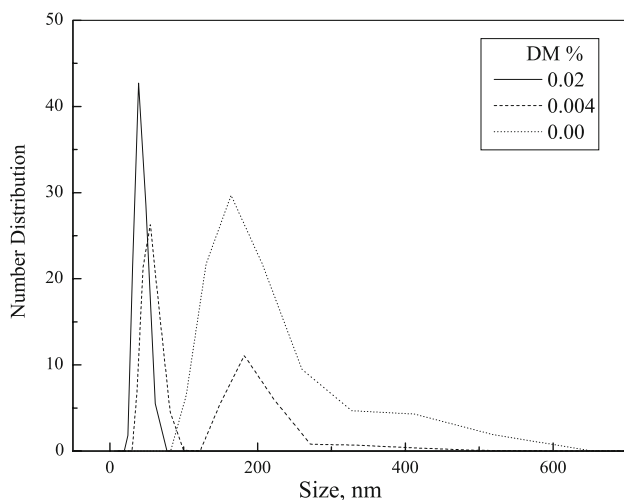


Fig. 3 Typical results from one of dynamic light scattering measurements using Malvern 3600 system

indicating the distinct excitation energy transfer pathways from chl *a* and xanthophyll molecules to the terminal emitters in aggregated samples. In separate isolations the spectral shape of aggregated LHC II differed too, maybe due to different plant material and/or differences in growth light regimes.

Previously, it was supposed that at intermediate DM concentrations, the samples contain a mixture of large and small aggregates (Barzda et al. 2001). To test this assumption the size of the aggregated samples was determined by a dynamic light scattering Malvern system using peak analysis by number. Typical results from one of the dynamic light scattering measurements are demonstrated in Fig. 3. The mean size (diameter) of trimeric forms (DM concentration 0.02%) was around 44 nm with width

22 nm. At intermediate DM concentration of 0.004% the complexes contained both large and small particles. The mean size of small particles in them was similar to that of trimers—52 nm with width 30 nm, and the size of large particles—185 nm with width 77 nm. In the samples without added detergent the mean size of large particles was around 190 nm with width 110 nm, nearly the same as the size of large particles in weakly aggregated complexes. Therefore, we can conclude that at intermediate DM concentrations the samples contain a mixture of large and small particles, the large particles being aggregated trimers, and the small ones—trimers.

The sizes obtained using dynamic light scattering look surprisingly large at first sight. All solubilization preparation procedures using detergents produce protein units covered by detergent and some lipids (Le Maire et al. 2000). Having in mind that the detergent used may form self-assembled layers on the surfaces with thickness as high as 11 nm (Mielczarski et al. 2004), it is easy to explain the obtained sizes, because our samples represent the so called “dressed” by the detergent micelles. The addition of glycerol would further enlarge their size as it was shown that the glycerol molecules have a tendency to agglomerate around the protein (Van Ghatty and Carri 2007).

As the samples at intermediate DM concentration contain a mixture of large and small particles, their total fluorescence spectrum might represent a sum of the spectra of the aggregated trimers and small aggregates. The equal size of the latter to the trimeric LHC II indicates that they have similar structure, thus supporting the previously made observation (Fig. 1b) that the spectral line shape of F680 in all samples is the same as that of the trimeric complexes, only slightly red-shifted.

The strong quenching and the appearance of a new emission band F700 upon aggregation implies that its emitter is located in aggregated trimers, whereas F680 is located in both small and large aggregates. Very recently van Oort et al. (2007b) have demonstrated that upon aggregation of trimeric LHC II a large amount of quenchers is created. The total spectrum of aggregated complexes consists of the two emission spectra of F680 and F700. Since the spectral line shape of F680 coincides with the shape of the slightly red-shifted spectrum of trimeric LHC II, subtracting its scaled spectrum from the total one should give the spectrum of F700, the putative quencher in large particles. The spectral shapes of F700 are compared in Fig. 4 under predominant excitation of chl *a*. They show that upon decreasing the detergent concentration the fluorescence of F700 also decreases. This should be due to the steeper decrease of lifetimes of quenching centers (van Oort et al. 2007b), since their relative number increases in large aggregates (Barzda et al. 2001). Having in mind that the fluorescence is proportional to the area

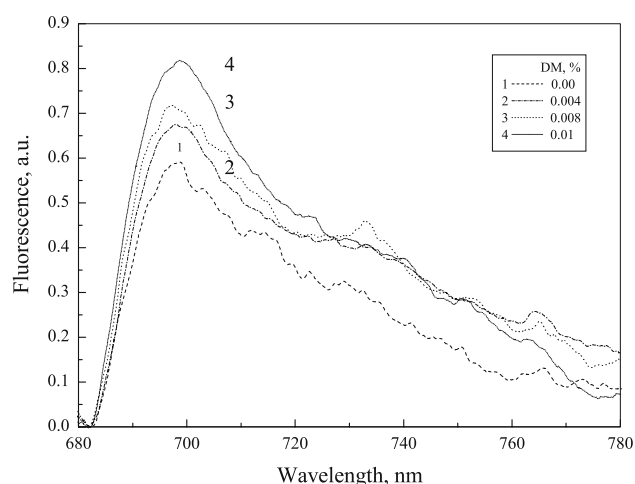


Fig. 4 The individual spectra of F700 in LHC II complexes in different aggregation states obtained after subtraction of the spectrum of trimeric LHC II from the spectra, shown in Fig. 1a

Table 1 Integrated fluorescence of F680, n_2 , and F700, n_3

DM (%)	n_2	n_3
0.020	171	0
0.010	35.1	35.8
0.008	24.75	33.7
0.004	23.5	31.9
0.000	14.8	25

under spectra, the areas under the scaled spectrum of trimeric LHC II and the spectrum of F700 will give their fluorescence, denoted as n_2 and n_3 , correspondingly. Their values are compared in Table 1.

Model for the chl *a* fluorescence quenching within LHC II with different degree of aggregation at low temperature (77 K)

On the basis of the analysis of the obtained data (Figs. 1, 3), we consider aggregated LHC II as a mixture of large and small particles, the spectral line shape of the latter coinciding with the trimeric one. Regardless of large heterogeneity in fluorescence lifetimes for different LHC II aggregates, the lifetime of the excited state in trimeric LHC II at 77 K is typically around 4.8 ns (Vasil'ev et al. 1997; Huyer et al. 2004; Palacios et al. 2002; Moya et al. 2001; Mullineaux et al. 1993; Barzda et al. 2000), a value, corresponding to that of monomeric chl *a* in different solvents (Huyer et al. 2004; Palacios et al. 2002). This fact shows that within the trimeric complexes the terminal fluorescence emitter is a monomeric chl *a*. Its intensity corresponds approximately to that of one chl molecule per

trimer—F680 (Peterman et al. 1994), and according to the latest crystal structure (Standfuss et al. 2005; Liu et al. 2004) it was assigned to chl *a* 612. Within large aggregates our experimental results: the highly fluorescence quenching (Fig. 1a), the appearance of a new emission band F700 (Fig. 1b), its red-shifted position and spectral line shape peaking at 698 nm (Fig. 4) suggest that F700 arises from a poorly fluorescing chlorophyll associate. The shorter fluorescence lifetime of the latter, being in the range between 0.1 and 0.85 ns (Pascal et al. 2005; Van Oort et al. 2007; Vasil'ev et al. 1997; Mullineaux et al. 1993) strongly supports our suggestion.

It was shown that upon aggregation the changes in the LHC II absorption spectrum are relatively small as compared to the changes in the fluorescence yield and kinetics (Ruban et al. 1997; Barzda et al. 2001; Gruszecki et al. 2006; Naqvi et al. 1997). This fact suggests that the quenching of fluorescence should be dynamic, influencing only the excited states of the emitters.

Based on the considerations above we suggested that in small aggregates and trimers the emitter is monomeric chlorophyll F680, whereas in large aggregates beside F680, the second emitter exists, chlorophyll associate with much lower quantum yield, denoted as F700. A schematic representation of energy pathways leading to population of first singlet excited states of emitting chl *a* forms F680 and F700 is illustrated in Fig. 5. It describes populations of antenna chlorophyll molecules in small aggregates and trimeric LHC II (subscript T, Fig. 5a) and in large aggregates (subscript A, Fig. 5b) in their ground, n_{0T} and n_{0A} , and first singlet excited, n_{1T} and n_{1A} , states, respectively. The populations of ground states of the two emitters, F680 and F700 are denoted as n_{02} and n_{03} , respectively. Their first singlet excited states, n_2 and n_3 , are mainly populated by energy transfer from antenna molecules. The populations of all considered states are normalized to the total chl

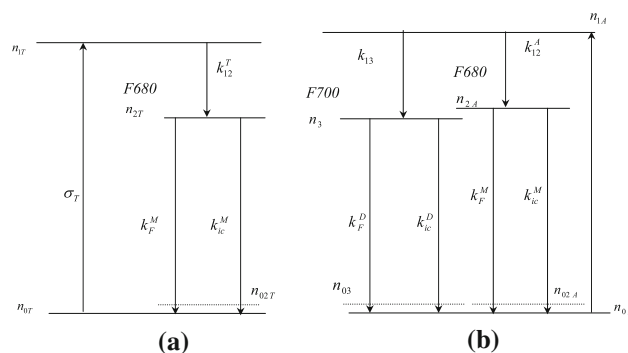


Fig. 5 Schematic representation of excitation energy pathways at 77 K (see text) leading to population of first singlet excited states of emitting chl *a* forms F680 and F700 in **a** trimeric and in small particles of LHC II and **b** in large particles

a concentration N_0 (i.e. $n_i = \frac{N_i}{N_0}$). The following processes are taken into account: ground absorption, excitation energy transfer to the emitters, and decays of excited states. The process of intersystem crossing is not considered because triplets are negligible upon excitation with the low-intensity light used. The kinetic contact between F680 and F700 is not considered either, because the distance between them being around 14 Å (Standfuss et al. 2005; Liu et al. 2004) is too long for efficient energy transfer as shown in Appendix 1.

Denoting the chl a absorption cross section as σ , it is obvious that:

$$\sigma = \sigma_A n_{0A} + \sigma_T n_{0T}. \quad (1)$$

Having in mind that $\sigma \approx \sigma_A \approx \sigma_T$ Eq. 1 becomes:

$$n_{0T} + n_{0A} = 1. \quad (1')$$

The rate constants for energy transfer from antenna chl molecules to the two emitters, F680 and F700, are denoted as k_{12} and k_{13} , respectively. Using Eq. 5 it is easy to calculate that the ratio of the rate constant in large aggregates, k_{12}^A , to the rate constant in trimers and small particles, k_{12}^T , is 1.24, having in mind that the average distance between the pigments in trimeric LHC II is 11.26 Å (Standfuss et al. 2005; Liu et al. 2004) and decreases with 0.4 Å upon aggregation of the complexes (Standfuss et al. 2005). This estimation enables us to assume that they are nearly equal.

The rate constant for fluorescence is denoted as k_F , being the same for chl monomer (M) and chl dimer (D) (see Appendix 2).

The model presented in Fig. 5 leads to five differential equations, described in Appendix 3:

Using the Eqs. 1 and 7'–11' the following relation between lifetimes of F680, τ_2 , and of F700, τ_3 , is deduced:

$$\tau_3/\tau_2 = n_3/(n_{2T}^T - n_2), \quad (2)$$

where $\tau_3 = \frac{1}{k_F + k_{ic}^D}$.

This relation makes it possible to draw the dependence of τ_3 on the detergent concentration using the experimental data summarized in Table 1, having in mind that the integrated fluorescence of F680 and F700 is proportional to n_2 and n_3 . The dependence is shown in Fig. 6 using the typical value of 4.8 ns for the lifetime of the excited state in trimeric LHC II (Vasil'ev et al. 1997; Hoyer et al. 2004; Palacios et al. 2002; Moya et al. 2001; Mullineaux et al. 1993). It clearly shows that the lifetime of F700 decreases upon aggregation reaching the value of 0.75 ns, approximate to the value, obtained by Pascal et al. (2005). The calculated dependence of τ_3 on the detergent concentration is in accordance with the explanation of the data presented in Fig. 4, given in the experimental data section. This dependence implies a strong increase of k_{ic}^D , the rate

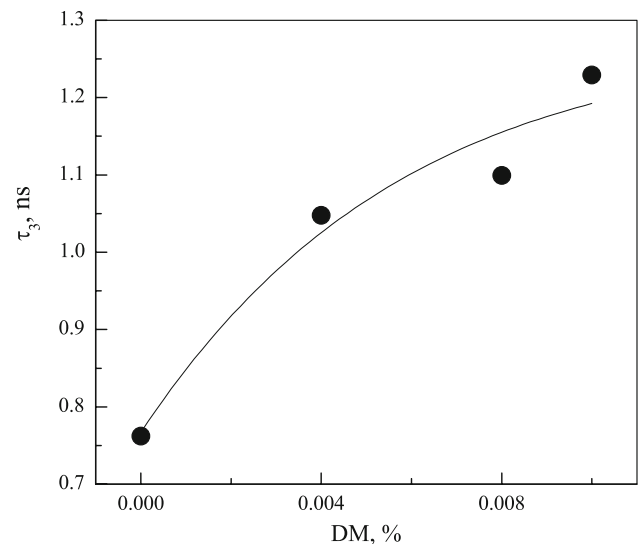


Fig. 6 The dependence of τ_3 on the detergent concentration. The filled circles present the results calculated from the experimental data in Table 1, using Eq. 2 and the typical value of 4.8 ns for the lifetime of the excited state in trimeric LHC II. The solid line is just guide for the eye

constant for internal conversion of F700, when decreasing the DM concentration. A possible reason for such a behavior of k_{ic}^D might be the formation of pigment multimers. As it was shown elsewhere (Liu et al. 2004; Wentworth et al. 2003; Pascal et al. 2005; Standfuss et al. 2005; Yan et al. 2007; Lampoura et al. 2002; Van Amerongen and van Grondelle 2001), the LHC II aggregation leads to changes in chl–chl and/or xanthophylls–chl interactions. The detergent-induced conformational changes of these complexes could bring two neighboring chl a molecules close together, forming a chl a dimer or eximer (Pascal et al. 2005; Van Oort et al. 2007a; Liu et al. 2004; Wentworth et al. 2003), or two chl a and one xanthophyll molecule, forming a hetero-trimer (Yan et al. 2007). The distance between the pigment molecules involved and their mutual orientation will change upon aggregation, modifying in this way the coupling strength between them. As a result, changes in k_{ic}^D will appear. These molecular associates, formed only in large aggregates and existing at detergent concentrations below the CMC, are situated, most probably, at the border between two LHC II trimers (Pascal et al. 2005; Liu et al. 2004; Yan et al. 2007).

Having in mind that the intensity of the fluorescence emitter in trimers and small aggregates corresponds approximately to that of one chl a molecule per trimer (Peterman et al. 1994), its concentration n_{02T} in ground state should be equal to the chl concentration in trimers, n_{0T} , divided by the known number of chl a molecules, l , in one trimer:

$$n_{02T} = n_{0T}/l. \quad (3)$$

If we assume that the quenchers are formed at the border of two trimers in large aggregates from two neighbor chl *a* molecules, as it was proposed (Liu et al. 2004; Wentworth et al. 2003; Yan et al. 2007) it follows that each couple of trimers in large aggregates should have one quencher, chl *a* associate. Hence, the relative concentration of quenchers, F700, n_{03} , can be expressed by the following equation:

$$n_{03} = n_{0A}/2l. \quad (4)$$

At intermediate DM concentrations, when complexes represent a mixture of large and small aggregates, the energy pathways are realized via both schemes shown in Fig. 5. Using Eqs. 1', 7'–11' and 2–4, the quadratic equations for the relative amount of chl molecules in their ground states in small and large aggregates can be deduced given in the Appendix 4 for n_{0A} . Using the obtained experimental data (Table 1) and Eq. 2 the solution for the amount of chl molecules in large aggregates, n_{0A} , enabled us to calculate its dependence on the detergent concentration. The dependence is shown in Fig. 7. As can be expected, the amount of chl molecules in large aggregates decreased steeply with the detergent concentration increase, correspondingly with the degree of disaggregation.

The value of l should coincide with the number of absorbing chl *a* molecules in one trimer—24 according to Standfuss et al. (2005) and Liu et al. (2004). Replacing this value in Eq. 4, the dependence for the amount of quenchers in large aggregates, F700, on the degree of aggregation are obtained, as shown in Fig. 8.

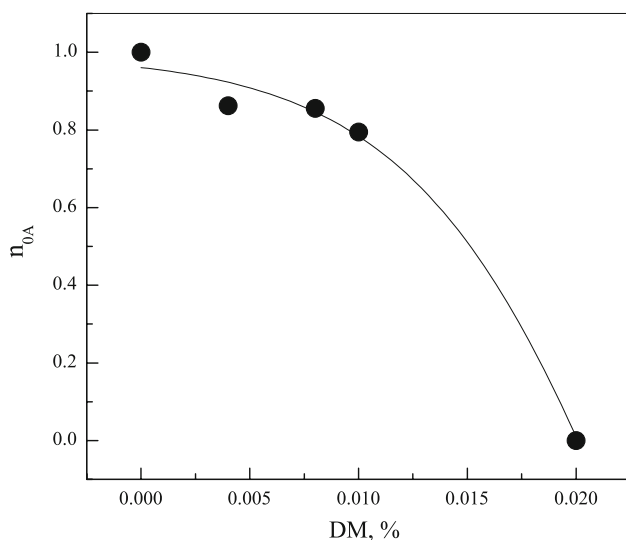


Fig. 7 The dependence of relative amount of chl *a* molecules in large aggregates in ground state on the detergent concentration. The filled circles present the results calculated from the experimental data in Table 1, using Eq. 14 and Eq. 2. The solid line is just guide for the eye

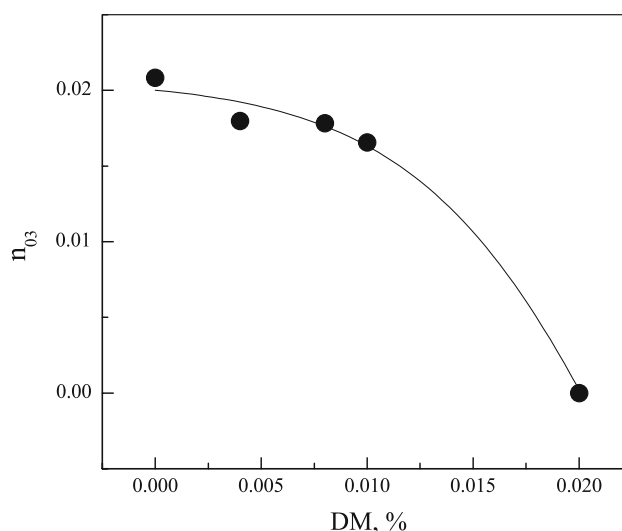


Fig. 8 The dependence of the amount of final emitters in large aggregates on the detergent concentration upon excitation with 436 nm. The filled circles present the results calculated from the data of Fig. 7 and using Eq. 4. The solid line is just guide for the eye

The dependencies obtained in the paper are based on the assumptions expressed by Eqs. 3 and 4 referring to an idealized case. Therefore, they must be considered as first approximated solutions of the system of Eqs. 1' and 7'–11'. To obtain solutions closer to the real case further experiments are needed to verify and justify the validity of the made assumptions. They are in course.

Conclusions

In this study evidences are presented that the preparations of tightly bound LHC II oligomers (Simidjiev et al. 1997) are heterogeneous and consisted of large and small particles (Fig. 3) with different fluorescence yield (Fig. 1). It is suggested that in small particles and trimers the emitter is monomeric chlorophyll, whereas in aggregated trimers there is also another emitter, which is a poorly fluorescing chlorophyll associate, emitting at 700 nm. Changes in the emission band of F700 are obtained (Fig. 4) evidencing that upon aggregation the decrease of the singlet excited-state lifetimes in LHC II is steeper than the increase of the quenching centers. A scheme for excitation energy pathways in LHC II in different aggregation states (Fig. 5) is proposed and a model, describing the populations of antenna chl molecules in small and large aggregates in their ground and first singlet excited states, is considered. The model offers an insight into molecular mechanism of fluorescence quenching giving us the possibility to obtain the dependencies of a relative amount of chl *a* molecules in ground state included in large and

small aggregates (Fig. 7) and the amount of final emitters in large and small aggregates (Fig. 8) on the detergent concentration. They revealed that upon aggregation the main reasons for the strong quenching of the chl *a* fluorescence are: (1) formation of large aggregates, (2) increasing of the relative amount of chl molecules forming these aggregates, (3) rise of the quencher's amount in large aggregates and the steep decrease of the lifetimes of the quenching centers in them.

The aggregation of LHC as pointed out in many studies (Jansson 2005; Pascal et al. 2005; Mullineaux et al. 1993; Ruban et al. 1997; Peterman et al. 1994; Wentworth et al. 2003; Horton et al. 2005) plays a key role in the NPQ mechanism of quenching the excess energy. The suggested mechanisms of quenching involved two ideas (Mullineaux et al. 1993; Horton et al. 2005; Van Oort et al. 2007a, b). The first one is that a small population of strongly quenched LHCs quenches fluorescence of connected LHCs (Mullineaux et al. 1993). The second is that the quenching is realized by local conformational changes of a large fraction of LHCs thereby with less strong quenching of individual LHC (Horton et al. 2005; Van Oort et al. 2007a, b). Our experimental results and proposed model reveal that the quenching could be performed by the series of processes leading to local conformational changes during aggregation, rise of the quencher's quantity and strong decrease of lifetimes of quenching centers. So, the quenching effect is enhanced due to the larger fraction of the aggregated state and the steep decrease of the singlet excited-state lifetimes in aggregated LHC II. In vivo, the combination of all those processes could take place in NPQ.

Acknowledgments This study was supported by Grant No. 11 (Program "Support for the research activities at the universities") from the Scientific Research Fund of the Ministry of Education and Science of Bulgaria and by Grant No. 16 from the Scientific Research Foundation at Sofia University, Bulgaria.

Appendix 1: Estimation of the ratio of the rate constants for excitation energy transfer from F680 to F700

It is well documented that the process of excitation energy transfer between the antenna pigments in green plants can be described with the localized Förster mechanism (Van Grondelle et al. 1994; Palacios et al. 2002) and the rate constant for excitation energy transfer is proportional to the minus sixth power of the distance between pigments:

$$k_{12} = \text{const } n^{-4} k^2 R^{-6}, \quad (5)$$

where n is the refraction index, k is the factor for orientation of the molecules and R is the distance between them.

It was shown that the average distance between the pigments in trimeric LHC II is 11.26 Å (Standfuss et al. 2005; Liu et al. 2004), whereas the distance between F680 and F700 is around 14 Å (Standfuss et al. 2005; Standfuss et al. 2005; Liu et al. 2004). Using Eq. 5 it is easy to calculate that the ratio of the rate constant for energy transfer between F680 and F700 to the average rate constant is 0.14, which enables us to neglect it in a first approximation.

Appendix 2: Evaluation of the rate constant for fluorescence

The rate constant for fluorescence k_F is given by:

$$k_F = \frac{1}{\tau_R} \approx \text{const} \tilde{\nu}_0^2 \varepsilon_{\max} \Delta \tilde{\nu}, \quad (6)$$

where τ_R is the chl *a* fluorescence lifetime, $\tilde{\nu}$ is the frequency in wavenumbers, $\Delta \tilde{\nu}$ is the full width at half maximum, $\tilde{\nu}_0$ is the wavenumber at the absorption maximum and ε_{\max} is the extinction coefficient at $\tilde{\nu}_0$. On the basis of the literature data (Shipman et al. 1976) about the values of $\tilde{\nu}_0 = 15,170 \text{ cm}^{-1}$, $\Delta \tilde{\nu} = 440 \text{ cm}^{-1}$ and $\varepsilon_{\max} = 84.9$ for monomeric chl *a* and $14,940 \text{ cm}^{-1}$, 720 cm^{-1} and 55.7 , respectively for dimeric chl *a*, the ratio of their fluorescence rate constants is estimated to be 0.96. Therefore, it is safe to assume that k_F is the same for chl monomers and chl dimers.

Appendix 3: Differential equations describing the chl *a* fluorescence quenching within LHC II with different degree of aggregation at low temperature (77 K)

The model (Fig. 5) leads to the following five differential equations:

$$\frac{dn_{1T}}{dt} = \sigma n_{0T} I - k_{12} n_{02T} n_{1T} / N_0 \quad (7)$$

$$\frac{dn_{2T}}{dt} = k_{12} n_{02T} n_{1T} / N_0 - (k_F + k_{ic}^M) n_{2T} \quad (8)$$

$$\frac{dn_{1A}}{dt} = \sigma n_{0A} I - k_{13} n_{03} n_{1A} / N_0 - k_{12} n_{02A} n_{1A} / N_0 \quad (9)$$

$$\frac{dn_3}{dt} = k_{13} n_{03} n_{1A} / N_0 - (k_F + k_{ic}^D) n_3 \quad (10)$$

$$\frac{dn_{2A}}{dt} = k_{12} n_{02A} n_{1A} / N_0 - (k_F + k_{ic}^M) n_{2A}, \quad (11)$$

where I is the intensity of excitation light and k_{ic} is the rate constant for internal conversion.

In steady state $\frac{dn_i}{dt} = 0$ and the Eqs. 7–11 become:

$$\sigma n_{0T} I = k_{12} n_{02T} n_{1T} / N_0 \quad (7')$$

$$k_{12}n_{02T}n_{1T}/N_0 = (k_F + k_{ic}^M)n_{2T} \quad (8')$$

$$\sigma n_{0A}I = k_{13}n_{03}n_{1A}/N_0 + k_{12}n_{02A}n_{1A}/N_0 \quad (9')$$

$$k_{13}n_{03}n_{1A}/N_0 = (k_F + k_{ic}^D)n_3 \quad (10')$$

$$k_{12}n_{02A}n_{1A}/N_0 = (k_F + k_{ic}^M)n_{2A} \quad (11')$$

At CMC, when all LHCs form trimers and $n_{0T} = 1$, the energy pathways are only realized via scheme shown in Fig. 5a. Therefore, the fluorescence is emitted only by F680. Its integrated fluorescence is denoted as n_{2T}^T , where superscript T means that all LHC II form trimers. Its value is easy to obtain from Eqs. 1' and 7':

$$n_{2T}^T = \sigma I \tau_2, \quad \text{where } \tau_2 = \frac{1}{k_F + k_{ic}^M}. \quad (12)$$

At intermediate DM concentrations, the total fluorescence emitted from F680 can be expressed as follows:

$$n_2 = n_{2T} + n_{2A} \quad (13)$$

Appendix 4: Equation for n_{0A}

The quadratic equation for the relative amount of chl molecules in their ground states in large aggregates, n_{0A} , obtained after the replaces using Eqs. 1', 7'–11' and Eqs. 2–4 is:

$$\frac{n_{2T}^T}{\tau_2} n_{0A}^2 + \left(\frac{n_2}{\tau_2} - \frac{2n_{2T}^T}{\tau_2} \right) n_{0A} + \frac{n_3}{\tau_3} = 0 \quad (14)$$

References

- Andreeva A, Stoitchkova K, Busheva M, Apostolova E (2003) The energy distribution between chlorophyll-protein complexes of thylakoid membranes from pea mutants with modified pigment content I. Changes due to the modified pigment content. *J Photochem Photobiol B* 70:153–162. doi:10.1016/S1011-1344(03)00075-7
- Barzda V, Vengris M, Valkunas L, van Grondelle R, van Amerongen H (2000) Generation of fluorescence quenchers from the triplet states of chlorophyll in major light-harvesting complex II from green plants. *Biochemistry* 39:10468–10477. doi:10.1021/bi992826n
- Barzda V, Gulbians V, Kananavicius R, Cervinskaskas V, van Amerongen H, van Grondelle R et al (2001) Singlet–singlet annihilation kinetics in aggregates and trimers of LHCII. *Biophys J* 80:2409–2421
- Boardman NK, Thorne SW (1971) Sensitive fluorescence method for the determination of chlorophyll *a*/chlorophyll *b* ratios. *Biochim Biophys Acta* 46181:222–231
- Cseh Z, Rajagopal S, Tsonev T, Busheva M, Papp E, Garab G (2000) Thermooptic effect in chloroplast thylakoid membranes. Thermal and light stability of pigment arrays with different levels of structural complexity. *Biochemistry* 39:15250–15257. doi:10.1021/bi001600d
- Finazzi G, Johnson GN, Dall'Osto L, Joliet P, Wollman F-A, Bassi R (2004) A zeaxanthin-independent nonphotochemical quenching mechanism localized in the photosystem II core complex. *Proc Natl Acad Sci USA* 101:12375–12380. doi:10.1073/pnas.0404798101
- Gilmore AM, Hazlett T, Govindjee (1995) Xanthophyll cycle-dependent quenching of photosystem II chlorophyll *a* fluorescence: formation of a quenching complex with a short fluorescence lifetime. *Proc Natl Acad Sci USA* 92:2273–2277. doi:10.1073/pnas.92.6.2273
- Grudziński W, Krupa Z, Garstka M, Maksymiec W, Swartz TE, Gruszecki WI (2002) Conformational rearrangements in light-harvesting complex II accompanying light-induced chlorophyll *a* fluorescence quenching. *Biochim Biophys Acta* 1554:108–117. doi:10.1016/S0005-2728(02)00218-9
- Gruszecki WI, Grudziński W, Gospodarek M, Patura M, Maksymiec W (2006) Xanthophyll-induced aggregation of LHCII as a switch between light-harvesting and energy dissipation systems. *Biochim Biophys Acta* 1757:1504–1511. doi:10.1016/j.bbabi.2006.08.002
- Hemerlrijk PW, Kwa LS, van Grondelle R, Dekker JP (1992) Spectroscopic properties of LHC-II, the main light-harvesting chlorophyll *a/b* protein complex from chloroplast membranes. *Biochim Biophys Acta* 1098:159–166. doi:10.1016/S0005-2728(05)80331-7
- Holt NE, Zigmantas D, Valkunas L, Li XP, Niyogi KK, Fleming GR (2005) Carotenoid cation formation and the regulation of photosynthetic light harvesting. *Science* 307:433–436. doi:10.1126/science.1105833
- Horton P, Ruban A, Walters R (1996) Regulation of light harvesting in green plants. *Annu Rev Plant Physiol Mol Biol* 47:655–684. doi:10.1146/annurev.arplant.47.1.655
- Horton P, Wentworth M, Ruban AV (2005) Control of the light harvesting function of chloroplast membranes: the LHCII-aggregation model for non-photochemical quenching. *FEBS Lett* 579:4201–4206. doi:10.1016/j.febslet.2005.07.003
- Huyer J, Eckert HJ, Irrgang KD, Miao J, Eichler HJ, Renger G (2004) Fluorescence decay kinetics of solubilized pigment protein complexes from the distal, proximal, and core antenna of Photosystem II in the range of 10–277 K and absence or presence of sucrose. *J Phys Chem* 108:3326–3334. doi:10.1021/jp0309441
- Jansson S (2005) A protein family saga: from photoprotection to light-harvesting (and back?). In: Demmig-Adams B et al (eds) *Photoprotection, photoinhibition, gene regulation and environment*, vol 21. Springer, Dordrecht, pp 145–153
- Krause GH, Briantais JM, Veronotte C (1983) Characterization of chlorophyll fluorescence quenching in chloroplasts by fluorescence spectroscopy at 77 K. *Biochim Biophys Acta* 723:169–175. doi:10.1016/0005-2728(83)90116-0
- Lampoura SS, Barzda V, Owen GM, Hoff AJ, van Amerongen H (2002) Aggregation of LHCII leads to a redistribution of the triplets over the central xanthophylls in LHCII. *Biochem* 41:9139–9144. doi:10.1021/bi025724x
- Le Maire M, Champeil P, Moller JV (2000) Interaction of membrane proteins and lipids with solubilizing detergents. *Biochim Biophys Acta* 1508:86–111. doi:10.1016/S0304-4157(00)00010-1
- Lichtenthaler HK (1987) Chlorophylls and carotenoids: Pigments of photosynthetic membranes. In: Colowick SP, Kaplan NO, Packer L, Dounce R (eds) *Methods Enzymol*, vol 148. Academic Press, pp 350–382
- Liu Z, Yan H, Wang K, Kuang T, Zhang J, An X et al (2004) Crystal structure of spinach major light-harvesting complex at 2.72 Å resolution. *Nature* 428:287–292. doi:10.1038/nature02373
- Mielczarski E, Mielczarski JA, Zhang L, Somasundaran P (2004) Structure of adsorbed *n*-dodecyl-β-D-maltoside layers on

- hematite. *J Colloid Interface Sci* 275:403–409. doi: [10.1016/j.jcis.2004.02.083](https://doi.org/10.1016/j.jcis.2004.02.083)
- Moya I, Silvestri M, Vallon O, Cinque G, Bassi R (2001) Time-resolved fluorescence analysis of the Photosystem II antenna proteins in detergent micelles and liposomes. *Biochemistry* 40:12552–12561. doi: [10.1021/bi010342x](https://doi.org/10.1021/bi010342x)
- Mullineaux CW, Pascal AA, Horton P, Holzwarth AR (1993) Excitation-energy quenching in aggregates of the LHC II chlorophyll-protein complex: a time-resolved fluorescence study. *Biochim Biophys Acta* 1141:23–28. doi: [10.1016/0005-2728\(93\)90184-H](https://doi.org/10.1016/0005-2728(93)90184-H)
- Naqvi KR, Melo TB, Raju BB, Javorfi T, Simidjiev I, Garab G (1997) Quenching of chlorophyll a singlets and triplets by carotenoids in light-harvesting complex of photosystem II: comparison of aggregates with trimers. *Spectrochim Acta Part A Mol Biomol Spectrosc* 53:2659–2667. doi: [10.1016/S1386-1425\(97\)00160-1](https://doi.org/10.1016/S1386-1425(97)00160-1)
- Palacios MA, De Weerd FL, Ihalaenen JA, van Grondelle R, van Amerongen H (2002) Superradiance and exciton (De)localization in light-harvesting complex II from green plants? *J Phys Chem* 106:5782–5787. doi: [10.1021/jp014078t](https://doi.org/10.1021/jp014078t)
- Pascal AA, Liu Z, Broess K, Van Oort B, van Amerongen H, Wang C et al (2005) Molecular basis of photoprotection and control of photosynthetic light-harvesting. *Nature* 436:134–137. doi: [10.1038/nature03795](https://doi.org/10.1038/nature03795)
- Peterman EJG, Dekker JP, van Grondelle R, van Amerongen H, Nussberger S (1994) Wavelength-selected polarized fluorescence of monomeric, trimeric, and aggregated light-harvesting complex II of green plants. *Lithuan J Phys* 34:301–306
- Ruban AV, Horton P (1992) Mechanism of Δ pH-dependent dissipation of absorbed excitation energy by photosynthetic membranes. I. Spectroscopic analysis of isolated light-harvesting complexes. *Biochim Biophys Acta* 1102:30–38. doi: [10.1016/0005-2728\(92\)90061-6](https://doi.org/10.1016/0005-2728(92)90061-6)
- Ruban AV, Calkoen F, Kwa SLS, van Grondelle R, Horton P, Dekker JP (1997) Characterization of LHCII in the aggregated state by linear and circular dichroism spectroscopy. *Biochim Biophys Acta* 1321:61–70. doi: [10.1016/S0005-2728\(97\)00047-9](https://doi.org/10.1016/S0005-2728(97)00047-9)
- Ruban AV, Pascal AA, Robert B, Horton P (2001) Configuration and dynamics of xanthophylls in light harvesting antennae of higher plants. *J Biol Chem* 276:24862–24870. doi: [10.1074/jbc.M103263200](https://doi.org/10.1074/jbc.M103263200)
- Shipman LL, Cotton TM, Norris JR, Katz JJ (1976) An analysis of the visible absorption spectrum of chlorophyll a monomer, dimer, and oligomers. *Am J Chem Soc* 98:8222–8230. doi: [10.1021/ja00441a056](https://doi.org/10.1021/ja00441a056)
- Simidjiev I, Barsda V, Mustardy L, Garab G (1997) Isolation of lamellar aggregates of the light-harvesting chlorophyll a/b protein complex of photosystem II with long-range chiral order and structural flexibility. *Anal Biochem* 250:169–175. doi: [10.1006/abio.1997.2204](https://doi.org/10.1006/abio.1997.2204)
- Standfuss J, van Scheltinga ACT, Lamborghini M, Kühlbrandt W (2005) Mechanisms of photoprotection and nonphotochemical quenching in pea light-harvesting complex at 2.5 Å resolution. *EMBO J* 24:919–928. doi: [10.1038/sj.emboj.7600585](https://doi.org/10.1038/sj.emboj.7600585)
- Van Amerongen H, van Grondelle R (2001) Understanding the energy transfer function of LHCII, the major light-harvesting complex of green plants. *J Phys Chem B* 105:604–617. doi: [10.1021/jp0028406](https://doi.org/10.1021/jp0028406)
- Van Ghattay PA, Carri G (2007) Dynamics of lysosome in a glycerol-water system. 2007 American Physical Society March Meeting, Denver, Colorado
- Van Grondelle R, Dekker JP, Gillbro T, Sundström V (1994) Energy transfer and trapping in photosynthesis. *Biochim Biophys Acta* 1187:1–65. doi: [10.1016/0005-2728\(94\)90166-X](https://doi.org/10.1016/0005-2728(94)90166-X)
- Van Oort B, van Hoek A, Ruban AV, van Amerongen H (2007a) Equilibrium between quenched and nonquenched conformations of the major plant light-harvesting complex studied with high-pressure time-resolved fluorescence. *J Phys Chem B* 111:7631–7637. doi: [10.1021/jp070573z](https://doi.org/10.1021/jp070573z)
- Van Oort B, van Hoek A, Ruban AV, van Amerongen H (2007b) Aggregation of Light-Harvesting Complex II leads to formation of efficient excitation energy traps in monomeric and trimeric complexes. *FEBS Lett* 581:3528–3532. doi: [10.1016/j.febslet.2007.06.070](https://doi.org/10.1016/j.febslet.2007.06.070)
- Vasil'ev S, Irrgang KD, Schotter T, Bergmann A, Eishler HJ, Renger G (1997) Quenching of chlorophyll a fluorescence in the aggregates of LHCII: steady state fluorescence and picosecond relaxation kinetics. *Biochemistry* 36:7503–7512. doi: [10.1021/bi9625253](https://doi.org/10.1021/bi9625253)
- Wentworth A, Ruban V, Horton P (2003) Thermodynamic investigation into the mechanism of the chlorophyll fluorescence quenching in isolated Photosystem II light harvesting complexes. *J Biol Chem* 278:21845–21850. doi: [10.1074/jbc.M302586200](https://doi.org/10.1074/jbc.M302586200)
- Yan H, Zhang P, Wang C, Liu Z, Chang W (2007) Two lutein molecules in LHCII have different conformations and functions: insights into the molecular mechanism of thermal dissipation in plants. *Biochem Biophys Res Commun* 355:457–463. doi: [10.1016/j.bbrc.2007.01.172](https://doi.org/10.1016/j.bbrc.2007.01.172)